

Chapter III

Analysis of Scattered Waves from Three Layers of Tree Trunk

3.1 Introduction

In Chapter II, the author has discussed about the analysis of the scattered wave from two layers of a tree trunk. The analysis was only focusing in two layers, but actually the tree trunk has three main layers (Kamal 1989). Hence in this study, the analysis of scattered wave from three layers of a tree trunk is discussed to explore the complex relationships of the radar backscattering mechanisms between microwaves and tropical vegetation types. Many researchers have developed electromagnetic modelling of vegetations (Kamal 1989, Li *et al.* 1999), but here the author attempts to develop a method to find the relationships between the radar backscattering coefficients and the characteristics of tropical forest vegetation, particularly species that are found in Indonesian tropical forests.

In this study, analysis of scattered wave from a tree trunk has been done in order to estimate the relationship between the diameter of a tree trunk and its backscattering coefficients S^o . In section 3.2, the modelling and formulation of scattering problems in three layers of a tropical tree trunk are discussed. Then the simulation of transverse electric (TE) wave propagation in a tropical tree trunk is done using the Finite Difference Time Domain (FDTD) method (Uno 1998, Yee 1966), where the Mur method (Mur 1981) is applied as the

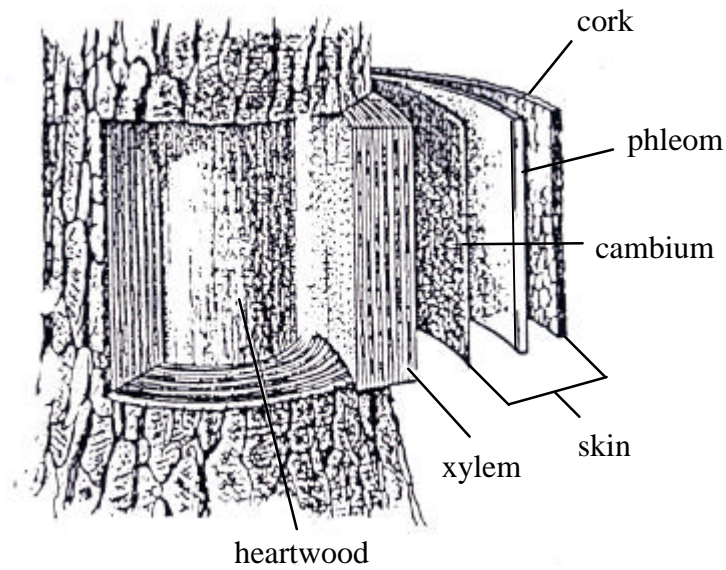


Figure 3.1. Tree trunk media

absorbing boundary condition to absorb the outgoing electromagnetic waves in a simulation space edges are discussed in section 3.3. In section 3.4, the analytical results are verified by comparing them with the simulated results. The application of the proposed method is discussed in section 3.5. Finally, conclusions are given in section 3.6.

3.2 Analysis

Actually, a tree trunk is composed of three media; skin, xylem, and heartwood, referring to figure 3.1 (Kamal 1989). Additionally, a skin medium is structured by cork, phleom and cambium layers. In this study, the scattering problems in a tropical tree trunk is discussed in order to investigate the correlation of backscattering coefficient S^o and the diameter of a tree trunk. This scattering problem in a tropical tree trunk is analysed by

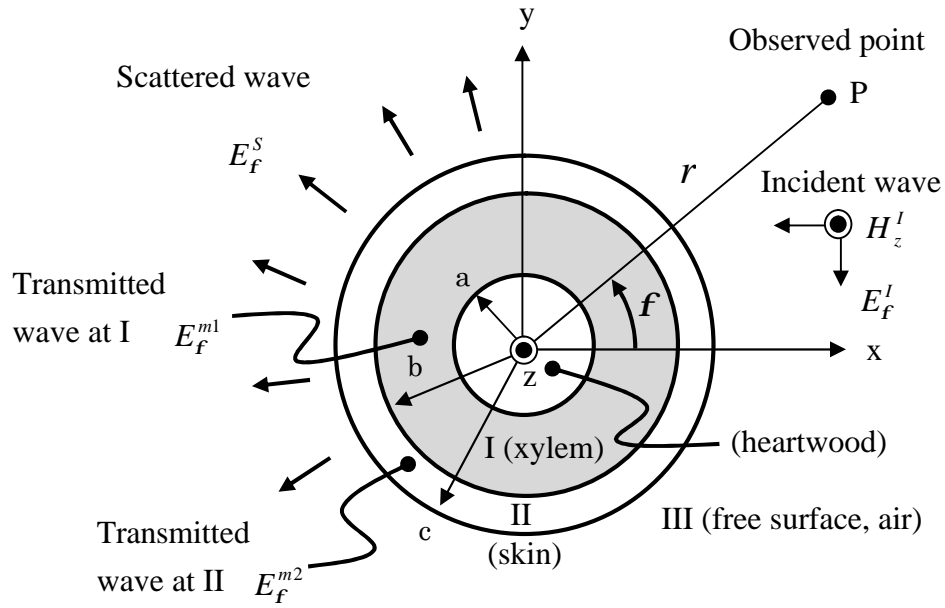


Figure 3.2. Geometry of analysis

deriving the scattered fields at each medium. The two-dimensional model of a tree trunk is shown in figure 3.2. Three layers of media compose this model of a tree trunk with infinite length in z-axis. The radii of heartwood, xylem and skin layer are a , b , and c , respectively. Where these radii have relations as $a=0.5c$ and $b=0.9c$.

In this study, the scattered wave from a tropical tree trunk is analysed. For this purpose, several trunks of tropical trees were collected and measured. The properties of xylem and skin are determined by \mathbf{e}_{r1} , \mathbf{m}_{r1} and \mathbf{e}_{r2} , \mathbf{m}_{r2} respectively. Where, \mathbf{e}_{ri} and \mathbf{m}_{ri} ($i=1, 2$) are complex dielectric constant and complex permeability, respectively. The water content of heartwood is high, consequently, heartwood may be assumed to be an infinite length of

perfect conductor or electromagnetic fields in heartwood is zero. Here, incident wave is assumed as a plane wave that has transverse electric (TE) mode and incident angle \mathbf{f} with respect to direction of observed point P from the origin of coordinate (0, 0). This wave propagates in $-x$ direction. Based on this figure, the \mathbf{f} component of the electromagnetic fields in a free space, xylem and skin are determined as

$$H_z^I = H_o^I e^{jk_o x} \quad (r > c) \quad (3.1)$$

$$H_z^S = H_o^I \sum_{m=0}^{\infty} b_m H_m^{(2)}(k_o r) \cos m\mathbf{f} \quad (r > c) \quad (3.2)$$

$$H_z^{m1} = H_o^I \sum_{m=0}^{\infty} \{a_{1m} J_m(k_1 r) + a'_{1m} N_m(k_1 r)\} \cos m\mathbf{f} \quad (a < r \leq b) \quad (3.3)$$

$$H_z^{m2} = H_o^I \sum_{m=0}^{\infty} \{a_{2m} J_m(k_2 r) + a'_{2m} N_m(k_2 r)\} \cos m\mathbf{f} \quad (b < r \leq c) \quad (3.4)$$

where the wave numbers of each medium are $k_1 = k_o \sqrt{\mathbf{m}_{r1} \mathbf{e}_{r1}}$ and $k_2 = k_o \sqrt{\mathbf{m}_{r2} \mathbf{e}_{r2}}$, and k_o is the wave number in free space. a_{1m} to b_m are amplitude coefficients. H_o^I is initial amplitude of incident magnetic field. J_m , N_m , and $H_m^{(2)}$ are m -th Bessel function, Neumann function, and 2nd kind of Hankel function. By referring to Appendix E, (3.1) is transformed to be

$$H_z^I = H_o^I \sum_{m=0}^{\infty} U_m J_m(k_o r) j^m \cos m\mathbf{f} \quad (r > c) \quad (3.5)$$

where

$$U_m = \begin{cases} 1, & m = 0 \\ 2, & m = 1, 2, \dots \end{cases} \quad (3.6)$$

By substituting (3.1) to (3.5) into source free Maxwell's equations below

$$\nabla \times \mathbf{H} = \mathbf{e} \frac{\partial \mathbf{E}}{\partial t} \quad (3.7)$$

the magnetic field of each medium is derived as

$$E_f^I = -\frac{k_o H_o^I}{j\omega \mathbf{e}_o} \sum_{m=0}^{\infty} U_m J'_m(k_o r) j^m \cos m\mathbf{f} \quad (r > c) \quad (3.8)$$

$$E_f^S = -\frac{k_o H_o^I}{j\omega \mathbf{e}_o} \sum_{m=0}^{\infty} b_m H_m^{(2)'}(k_o r) \cos m\mathbf{f} \quad (r > c) \quad (3.9)$$

$$E_f^{m1} = -\frac{k_1 H_o^I}{j\omega \mathbf{e}_1} \sum_{m=0}^{\infty} \{a_{1m} J'_m(k_1 r) + a'_{1m} N'_m(k_1 r)\} \cos m\mathbf{f} \quad (a < r \leq b) \quad (3.10)$$

$$E_f^{m2} = -\frac{k_2 H_o^I}{j\omega \mathbf{e}_2} \sum_{m=0}^{\infty} \{a_{2m} J'_m(k_2 r) + a'_{2m} N'_m(k_2 r)\} \cos m\mathbf{f} \quad (b < r \leq c) \quad (3.11)$$

Further, by substituting (3.1) to (3.5) and (3.8) to (3.11) into the boundary condition of each interface between media given below:

$$r = a \quad E_f^{m1} = 0 \quad (3.12)$$

$$r = b \quad E_f^{m1} = E_f^{m2} \quad \text{and} \quad H_z^{m1} = H_z^{m2} \quad (3.13)$$

$$r = c \quad E_f^{m2} = E_f^S + E_f^I \quad \text{and} \quad H_z^{m2} = H_z^S + H_z^I \quad (3.14)$$

the amplitude coefficient b_m of scattered wave from tree trunk E_f^S is obtained as;

$$b_m = -\frac{U_m j^m [\mathbf{a}_{6m} J_m(k_o c) - \mathbf{a}_{7m} J'_m(k_o c)]}{\mathbf{a}_{6m} H_m^{(2)'}(k_o c) - \mathbf{a}_{7m} H_m^{(2)}(k_o c)} \quad (3.15)$$

where

$$\mathbf{a}_{1m} = \frac{N'_m(k_1 a)}{J'_m(k_1 a)} \quad (3.16)$$

$$\mathbf{a}_{2m} = N'_m(k_1 b) - \mathbf{a}_{1m} J'_m(k_1 b) \quad (3.17)$$

$$\mathbf{a}_{3m} = N_m(k_1 b) - \mathbf{a}_{1m} J_m(k_1 b) \quad (3.18)$$

$$\mathbf{a}_{4m} = \frac{k_1}{\mathbf{e}_1} \mathbf{a}_{2m} J_m(k_2 b) - \frac{k_2}{\mathbf{e}_2} \mathbf{a}_{3m} J'_m(k_2 b) \quad (3.19)$$

$$\mathbf{a}_{5m} = \frac{k_1}{\mathbf{e}_1} \mathbf{a}_{2m} N_m(k_2 b) - \frac{k_2}{\mathbf{e}_2} \mathbf{a}_{3m} N'_m(k_2 b) \quad (3.20)$$

$$\mathbf{a}_{6m} = \frac{k_2 \mathbf{e}_o}{k_o \mathbf{e}_2} \left\{ N'_m(k_2 c) - \frac{\mathbf{a}_{5m}}{\mathbf{a}_{4m}} J'_m(k_2 c) \right\} \quad (3.21)$$

$$\mathbf{a}_{7m} = N_m(k_2 c) - \frac{\mathbf{a}_{5m}}{\mathbf{a}_{4m}} J_m(k_2 c) \quad (3.22)$$

Finally, by substituting the amplitude coefficient b_m of (3.15) into (3.9), the scattered electric field is obtained.

In the same manner, transverse magnetic (TM) mode of scattered waves from three layers of tree trunk was derived as Appendix B. The electric fields in each medium will be

$$\text{Incident wave} \quad E_z^I = E_o^I \sum_{m=0}^{\infty} U_m J_m(k_o r) j^m \cos m\mathbf{f} \quad (r > c) \quad (3.23)$$

$$\text{Scattered wave} \quad E_z^S = E_o^I \sum_{m=0}^{\infty} b_m H_m^{(2)}(k_o r) \cos m\mathbf{f} \quad (r > c) \quad (3.24)$$

$$\text{Medium I} \quad E_z^{m1} = E_o^I \sum_{m=0}^{\infty} \{a_{1m} J_m(k_1 r) + a'_{1m} N_m(k_1 r)\} \cos m\mathbf{f} \quad (a < r \leq b) \quad (3.25)$$

$$\text{Medium II} \quad E_z^{m2} = E_o^I \sum_{m=0}^{\infty} \{a_{2m} J_m(k_2 r) + a'_{2m} N_m(k_2 r)\} \cos m\mathbf{f} \quad (b < r \leq c) \quad (3.26)$$

and the magnetic fields will be

$$\text{Incident wave} \quad H_f^I = \frac{k_o E_o^I}{j\omega \mathbf{m}_o} \sum_{m=0}^{\infty} U_m J'_m(k_o r) j^m \cos m\mathbf{f} \quad (r > c) \quad (3.27)$$

$$\text{Scattered wave} \quad H_f^S = \frac{k_o E_o^I}{j\omega \mathbf{m}_o} \sum_{m=0}^{\infty} b_m H_m^{(2)'}(k_o r) \cos m\mathbf{f} \quad (r > c) \quad (3.28)$$

$$\text{Medium I} \quad H_f^{m1} = \frac{k_1 E_o^I}{j\omega \mathbf{m}_1} \sum_{m=0}^{\infty} \{a_{1m} J'_m(k_1 r) + a'_{1m} N'_m(k_1 r)\} \cos m\mathbf{f} \quad (a < r \leq b) \quad (3.29)$$

$$\text{Medium II} \quad H_f^{m2} = \frac{k_2 E_o^I}{j\omega \mathbf{m}_2} \sum_{m=0}^{\infty} \{a_{2m} J'_m(k_2 r) + a'_{2m} N'_m(k_2 r)\} \cos m\mathbf{f} \quad (b < r \leq c) \quad (3.30)$$

By substituting these fields into the boundary conditions, the amplitude coefficient b_m is obtained as

$$b_m = \frac{U_m j^m \{ \mathbf{a}_{6m} J'_m(k_o c) - \mathbf{a}_{7m} J'_m(k_o c) \}}{\mathbf{a}_{7m} H_m^{(2)'}(k_o c) - \mathbf{a}_{6m} H_m^{(2)}(k_o c)} \quad (3.31)$$

Table 3.1. Dielectric constants of Indonesian tropical forest trees at the frequency of

JERS-1 SAR ($f = 1.275$ GHz)

species names	skin ($\mathbf{e}_{r2} = \mathbf{e}'_r - j\mathbf{e}''_r$)		xylem ($\mathbf{e}_{r1} = \mathbf{e}'_r - j\mathbf{e}''_r$)	
	\mathbf{e}'_r	\mathbf{e}''_r	\mathbf{e}'_r	\mathbf{e}''_r
teak	3.1	0.4	11.5	2.6
mahogany	2.7	0.3	10.2	2.1
pine	3.4	0.4	13.6	3.0
rasamala	2.5	0.3	9.4	2.1

where the constants of (3.31) can be referred in Appendix B.

The dielectric constant \mathbf{e}_r of several sample of tree trunks were measured experimentally using dielectric probe kit HP85070B (figure 1.6.(a)), and the results are shown in figure 1.8 and table 3.1 which shows dielectric constants in frequency $f = 1.275$ GHz (JERS-1 SAR).

3.3 Simulation

In this study, the author considers the scattered waves from tropical tree trunk to explore the relationship between backscattering coefficient \mathbf{s}^o and the diameter of three layers of tree trunk. The finite-difference model (Yee 1966) is implemented in two dimensions (2-D) as shown in figure 3.3. In this figure, simulation space is sampled into $INX \times INY$ grids.

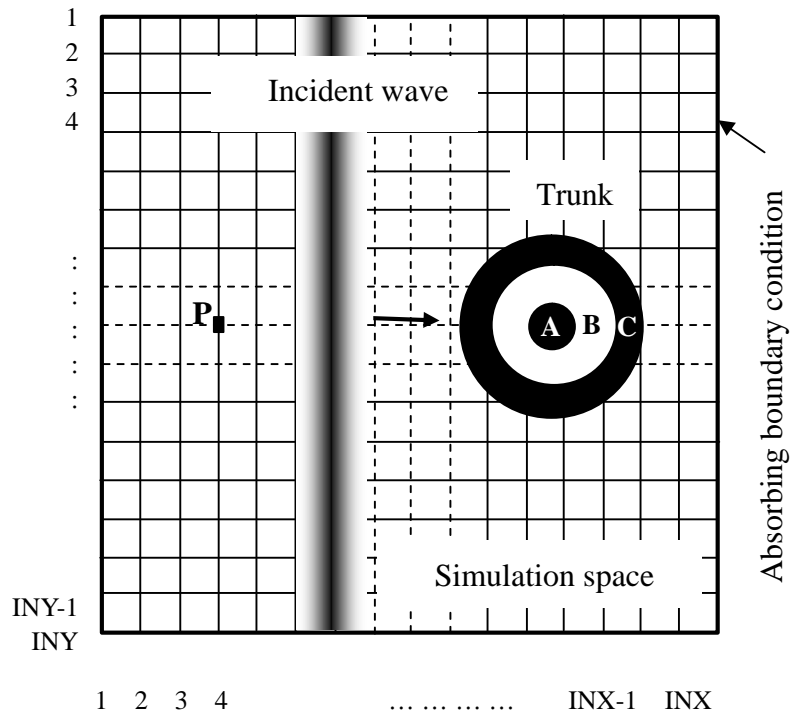


Figure 3.3. Geometry of simulation space. Remarks: P is observed point. A, B and C are heartwood, xylem, and skin, respectively. Simulation space is divided into INX x $IN Y$ grids of meshes.

Referring to the simulation in Chapter II with the same parameters, i.e. incident pulse using Gaussian pulse, boundary condition using Mur method (Mur 1981). Finally, the two dimensional backscattering coefficient \mathbf{s}^o is defined by (3.32), where E_y^l is observed electric field intensity on the trunk surface in frequency $f = 1.275 \text{ GHz}$.

$$\mathbf{s}^o = \frac{2pR}{l} \left(\frac{\langle |E_y^s|^2 \rangle}{\langle |E_y^l|^2 \rangle} \right)_{f=1.275 \text{ GHz}} \quad (3.32)$$

Where R is distance from centre of tree trunk to the observation point. l is effective scattered surface of tree trunk, in this case, is assumed as pb . In the calculation of its backscattering coefficient in the analysis, E_y^s and E_y^l are equal to E_f^s and E_f^l respectively at incident angle 0° .

3.4. Results

In simulation space, see figure 3.3, scattered wave from an infinite length of tree trunk is considered. This tree trunk is composed of three media; skin, xylem, and heartwood. The radius of tree trunk varies from 0 to 40 grids (or 0 to 0.5m). The simulation space edges (external boundaries) are surrounded by artificial absorbing boundary condition (Mur method), refer the simulation in Chapter II. Incident wave is a plane wave with intensity as shown by Gaussian pulse, which propagates from left to right of the simulation space in speed of light. Parameter of simulation is simulation space grids $INX = INY = 300$,

space-increments $\Delta x = \Delta y = 1.25 \times 10^{-2}$ m, time-increment $\Delta t = 2.5 \times 10^{-11}$ s, maximum intensity of initial electric field 100 V/m, and running time $t = 600\Delta t$ s. Figure 3.4 shows scattered wave from tree trunk with $t = 50\Delta t$ to $300\Delta t$ s. Additionally, figure 3.5 shows details of scattered wave when $t = 300\Delta t$ s, where A, B, C, and D are scattered waves from skin, xylem, heartwood, and forwarded wave that is occurred by clipping wave on the tree trunk surface, respectively. Then E, F, and G are skin, xylem, and heartwood, respectively. The observed point P is at 1.5 m from centre of tree trunk. This point is used to observe intensities of scattered electromagnetic fields.

In this study, the author observed only the horizontal component (TE wave) or electric field E_y^S in backscattering direction ($\boldsymbol{f} = 0^\circ$). The backscattered electric field is computed and is shown in figure 3.6. In this figure, A, B, and C show scattered waves from skin, xylem, and heartwood, respectively. Further, fast Fourier Transform is employed to obtain power spectrum of it and electric field intensity of preferred frequency, in this case, frequency of Japanese Earth Resources Satellite (JERS-1) SAR, $f = 1.275$ GHz was used. Finally, the backscattering coefficient is calculated using (3.32) and the result is shown in figure 3.7 (\diamond - simulation).

In the analysis, direction of incident wave is the same as of observed point P or $\boldsymbol{f} = 0^\circ$. Consequently, E_f^S is equivalent to E_z^S that obtained in simulation where the distance between the centre of tree trunk to the observed point is 1.5 m. By considering the

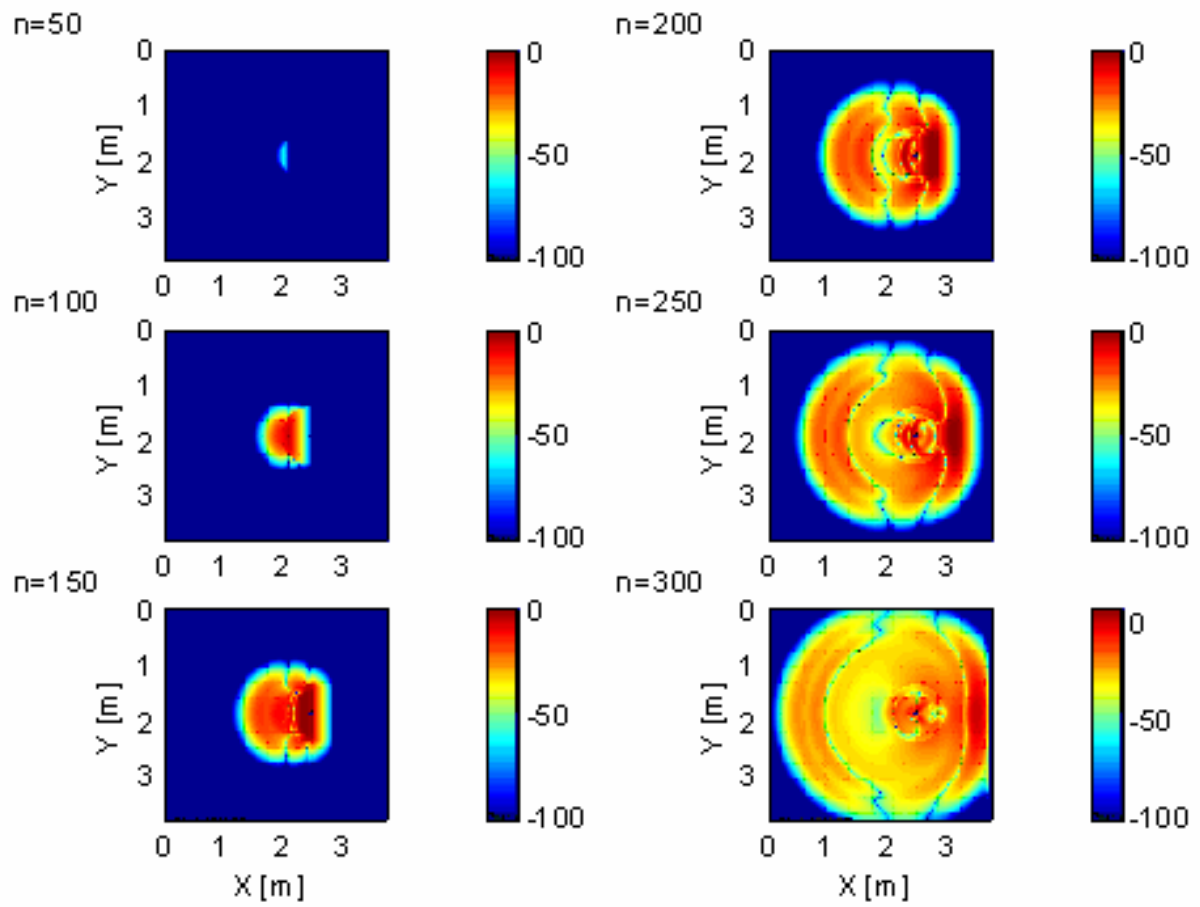


Figure 3.4. Distribution of scattered electric field intensity E_y^s with $t = 50\Delta t$ to $300\Delta t$ s.

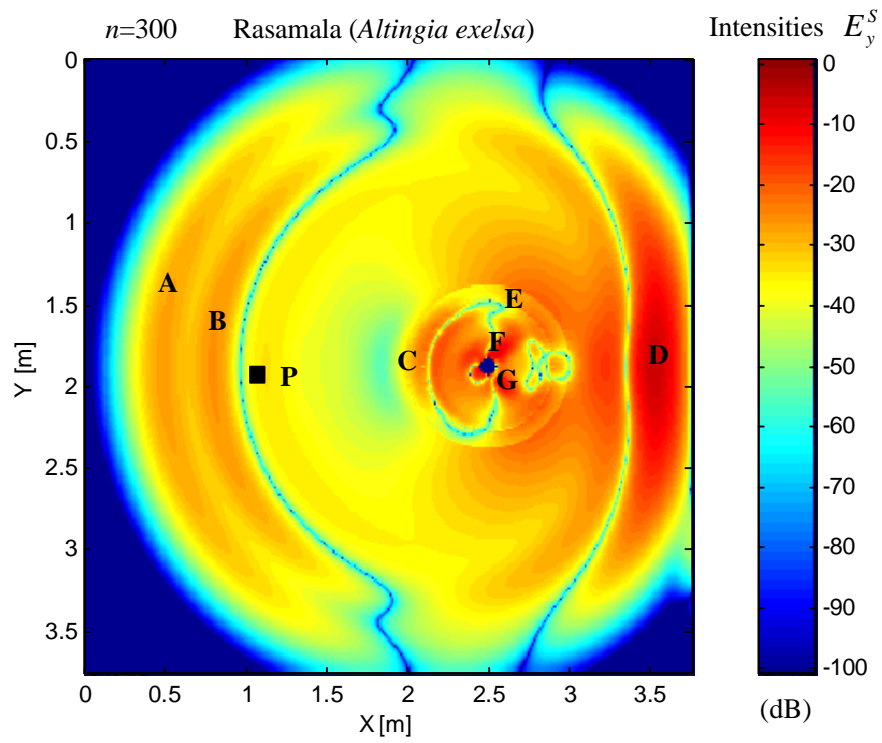


Figure 3.5. Distribution of scattered electric field E_y^S in $t = 300\Delta t$ s, where A, B and C are scattered wave from skin, xylem and heartwood, respectively. P is observed point. E, F and G are skin, xylem and heartwood, respectively. D is forwarded wave that is occurred by clipping wave that flows on the trunk surface and scattered to the backward of tree trunk.

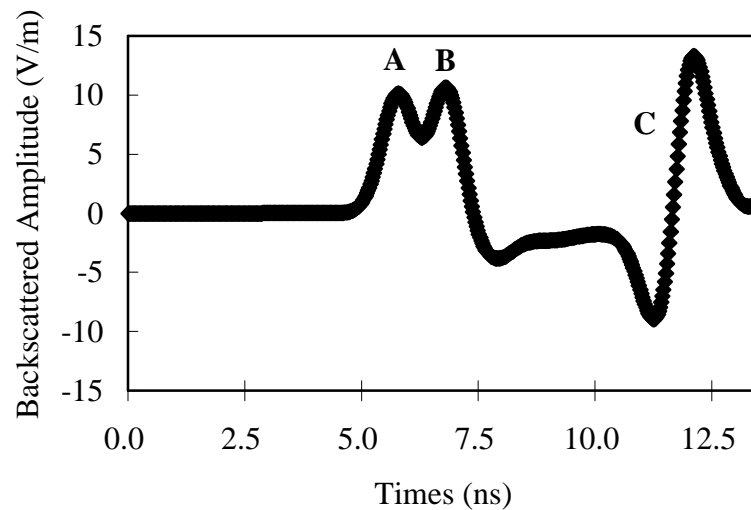


Figure 3.6. Scattered electric field intensities at observed point P. A, B and C are scattered pulse from skin, xylem and heartwood, respectively.

parameter of JERS-1 SAR, the result of analysis is obtained and is shown in figure 3.7 (◆ - rasamala). This result is obtained from the analysis of scattered wave from a tree trunk of rasamala (*Altingia exelsa*) in analysis area. The analysis result compares well with simulation ones. However, a small error was found. It can be considered that the error is generated by the FDTD calculation error caused by calculation using the sampled grids. Additionally, in the same figure, the results of analysis for teak (*Tectona grandis*), pine (*Pinus merkusii*), and mahagony (*Swietenia macrophylla*) are depicted too.

From these results we know that the increment of tree trunk diameter was directly proportional to increment of the backscattering coefficient. It means that backscattering is influenced by the width of tree trunk surface and volume of it. When the surface is wide, the

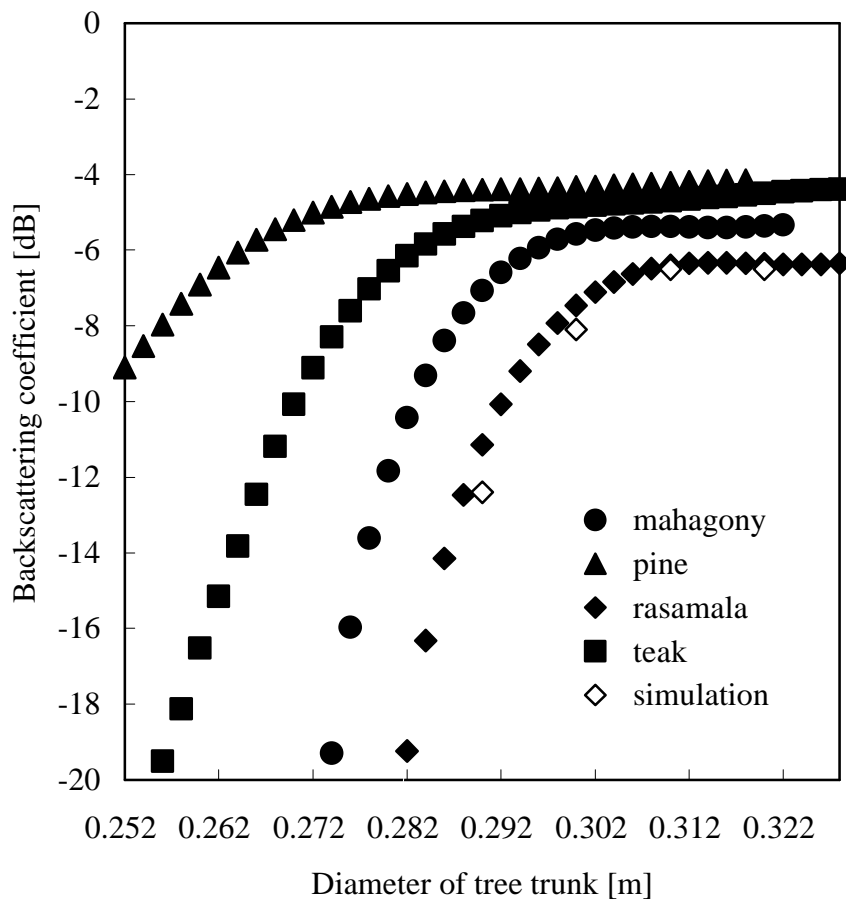


Figure 3.7. Analysis and simulation results for four species of Indonesian tropical forest, where the diameter of tree trunk is equal with $2c$, where c is radius of tree trunk.

reflected or scattered field intensity or energy will be higher, and in the contrary of it.

The application of this study will be applied to monitor *rasamala* (*Altingia exelsa*) species that is mainly distributed around Gede Pangrango National Park, west Java, Indonesia using JERS-1 Synthetic Aperture Radar (SAR, L band) data. The application will be discussed in the next section.

3.5. Application

3.5.1 Study area

The study area was Cisarua tropical forest, part of Gede Pangrango National Park, west Java, Indonesia (part of A area in figure 3.8 and 3.9). Figure 3.8 and 3.9 show JERS-1 Visible Near Infra Red (VNIR) and Synthetic Aperture Radar (SAR) data respectively that acquired at the same area (Path 107 Row 312) on 30 September 1997 and 10 August 1997. This area is one of the wettest parts of Java with an average annual rainfall of around 3000mm to 4200mm, while the relative humidity varies between 80% and 90%. Figure 3.10 shows the altitude distribution of the study area where the study area has altitude ranging from 627m to 2030m as seen in figure 3.11 (DEM 1990). Biomes of this area are the sub-montane (1100m to 1500m) and montane (1500m to 2030m) tropical forest. In addition to that, settlement and dry paddy fields called *ladang* are distributed in the region with altitude between 627m and 1100m above sea level (asl). Tea, which has tall canopy about 1m, is usually planted at

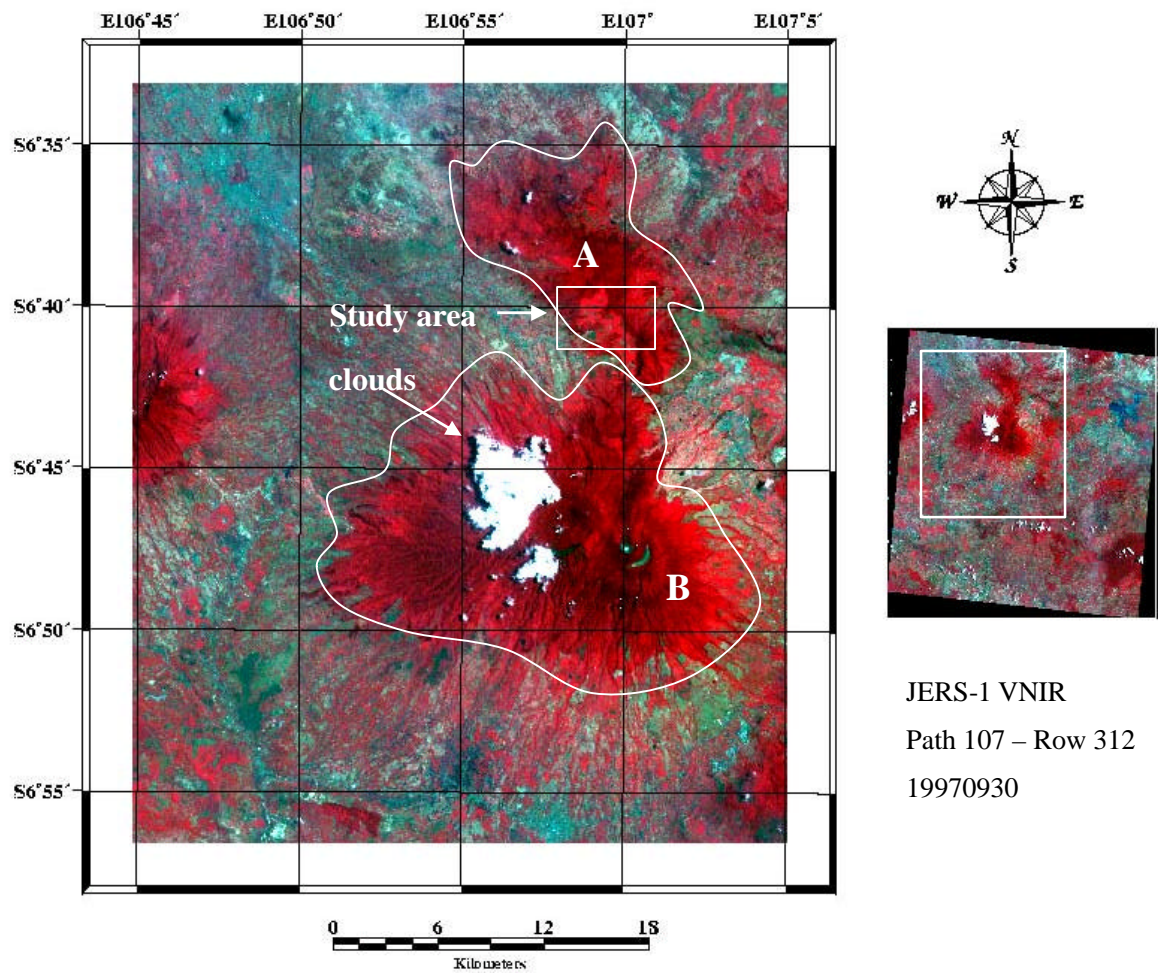


Figure 3.8. JERS-1 VNIR data of the study area (Path 107 Row 312, 19970930): Gede Pangrango National Park, west Java, Indonesia. Remark: A and B show northern and southern part of the National Park, respectively.

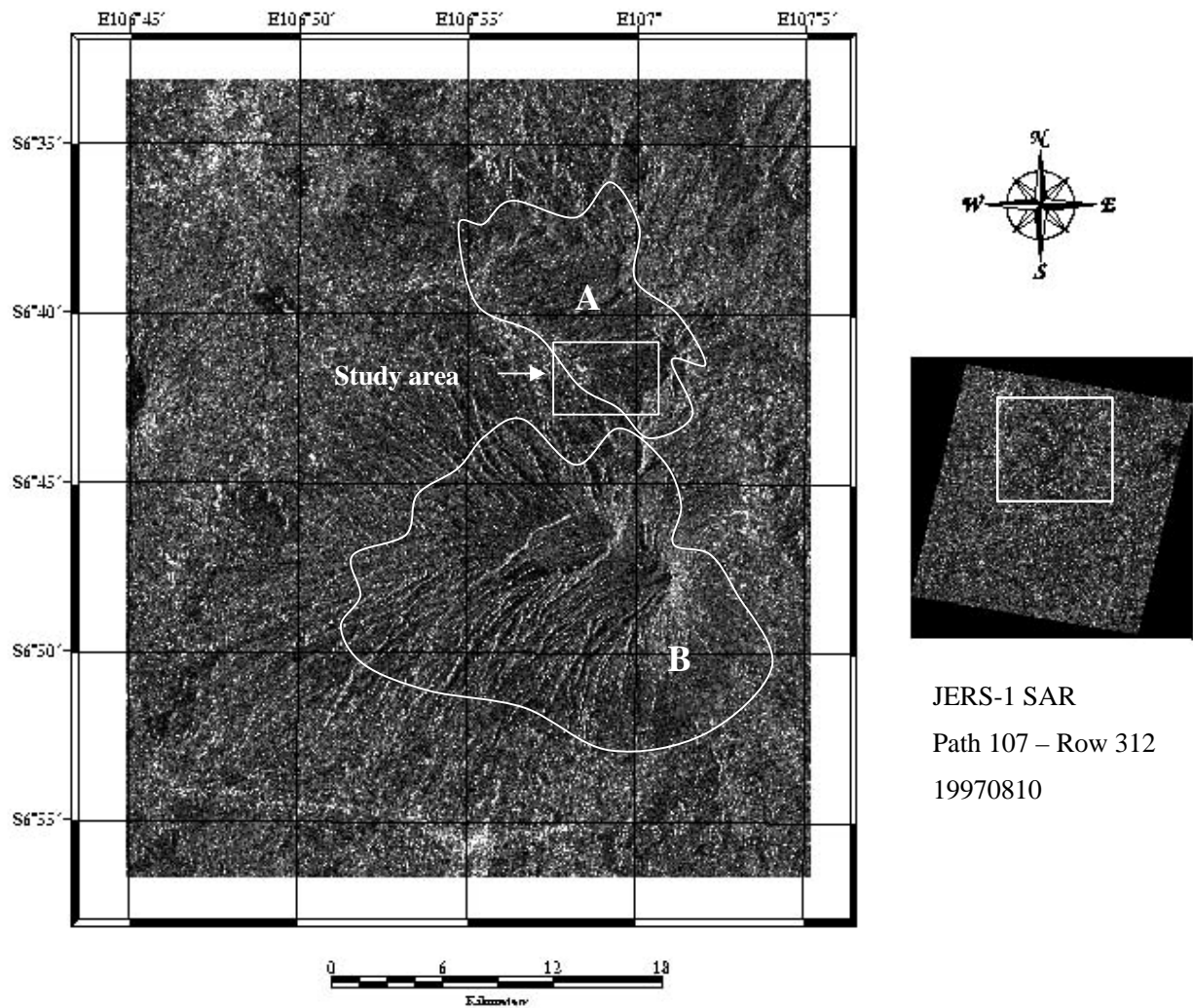


Figure 3.9. JERS-1 SAR data of the study area (Path 107 Row 312, 19970810): Gede Pangrango National Park, west Java, Indonesia. Remark: A and B show northern and southern part of the National Park, respectively.

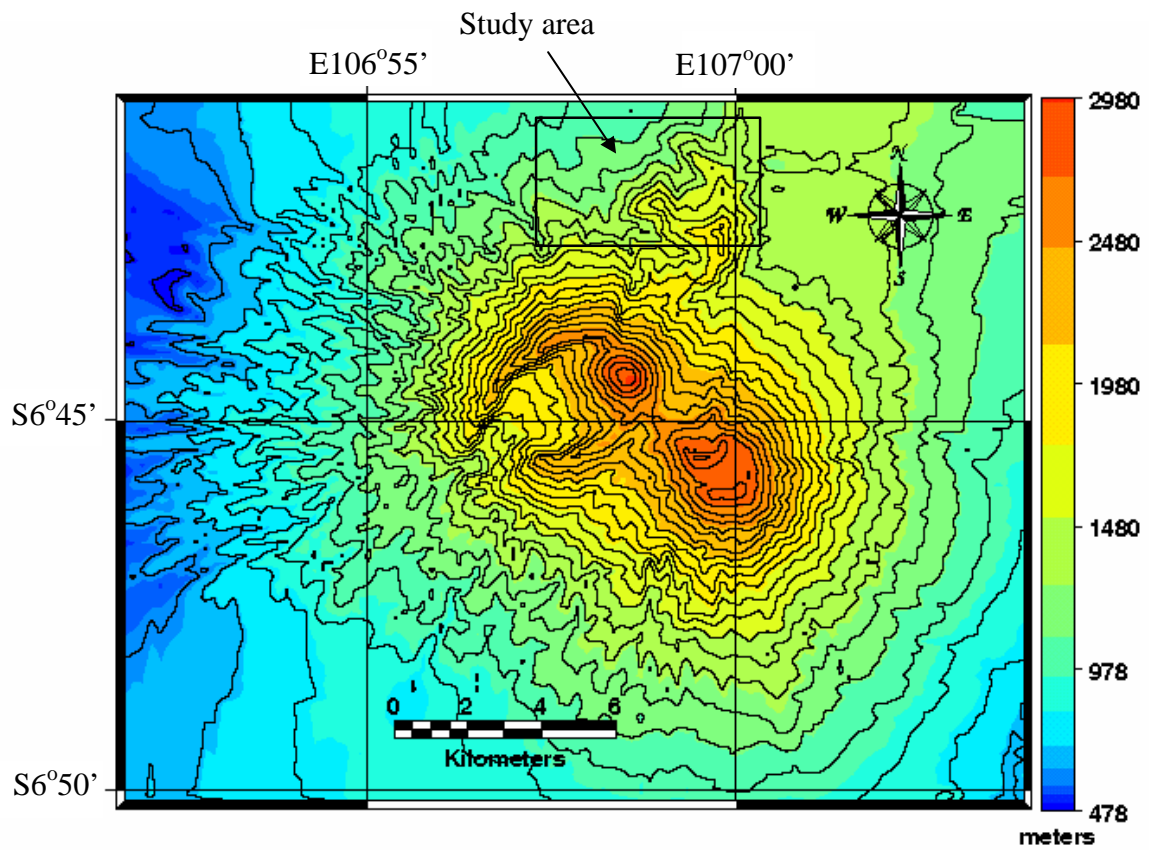


Figure 3.10. Altitude distribution of the study area : Mount Gede Pangrango National Park, west Java, Indonesia.

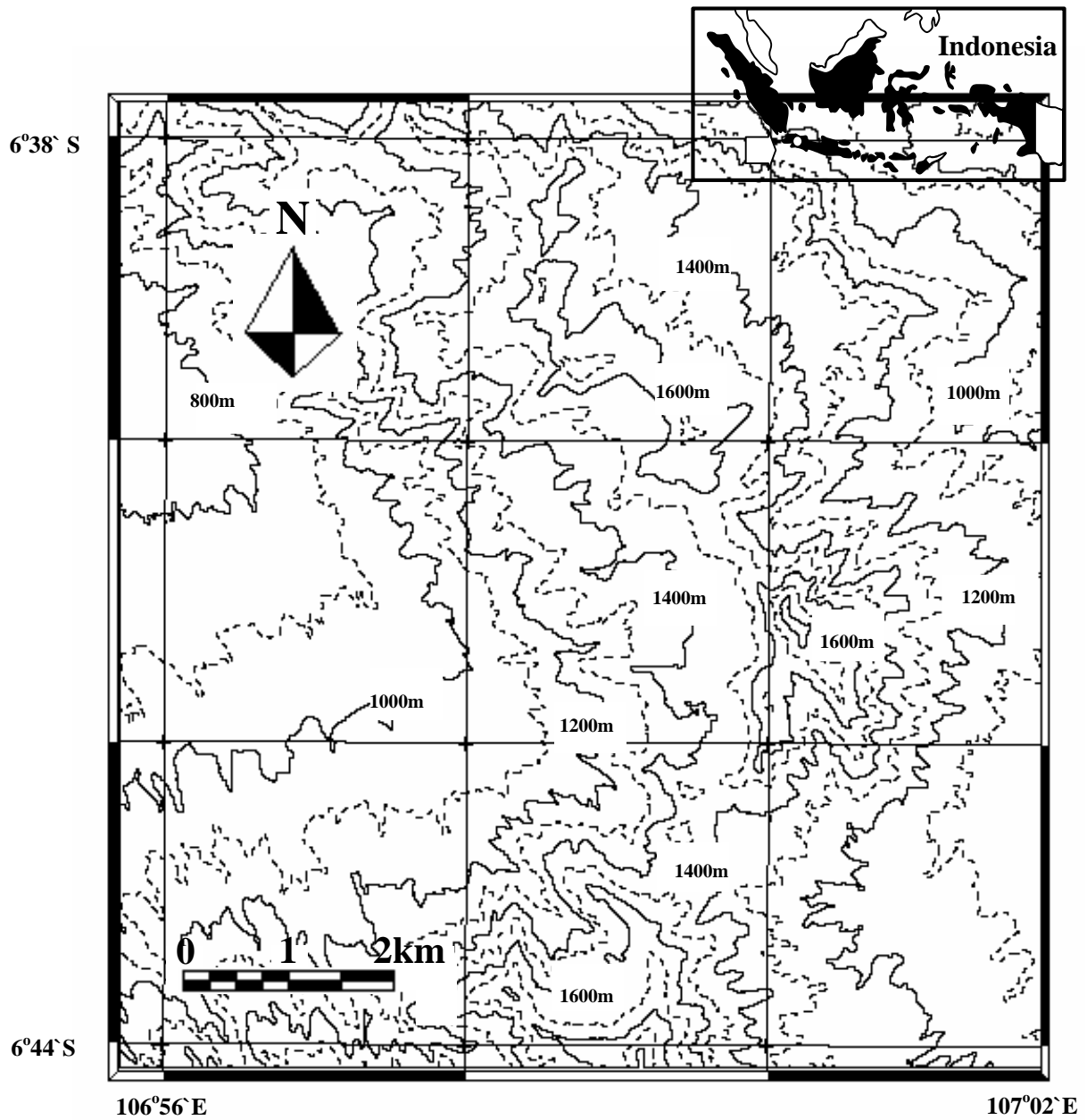


Figure 3.11. Location of the study area: Gede Pangrango National Park (part of area A in figure 3.8 and 3.9)

altitude between 627m and 2030m by government companies. Appendix F shows part of the ground data of the study area. The sub-montane tropical forest has the highest diversity of plant life and is characterized by large trees forming diameter trunks between 0.2m and 0.4m. The dominant species in this ecosystem is rasamala (*Altingia exelsa*). Besides a rich ground flora containing begonias and ferns, many species of epiphytes are found growing non-parasitically on twigs and branches (e.g. orchids, lianas, and herbs).

Montane tropical forest has a lower diversity of plants with fewer herb species than the sub-montane zone. Common trees included rasamala; also noticeable are puspa (*Schima walichii*) and conifers (*Dacrycarpus imbricatus* and *Podocarpus neriifolius*).

3.5.2 Data processing

The JERS-1 SAR data (figure 3.9) was examined in order to estimate the diameters of rasamala in the study area. The data (path 107, row 312) was acquired on 10 August 1997 during the dry season in the study area. This data was processed at level 2.1 or standard geocoded data and was resampled to Universal Transverse Mercator (UTM) projection by the Earth Observation Research Centre (EORC) of National Space Development Agency (NASDA) of Japan. Firstly, a 3x3 median filter was employed and the second process used a 5x5 average filter to reduce inherent speckle noise (Sunar *et al.* 1998). At the same time, the image was also referenced to the UTM co-ordinate system, through a polynomial rectification

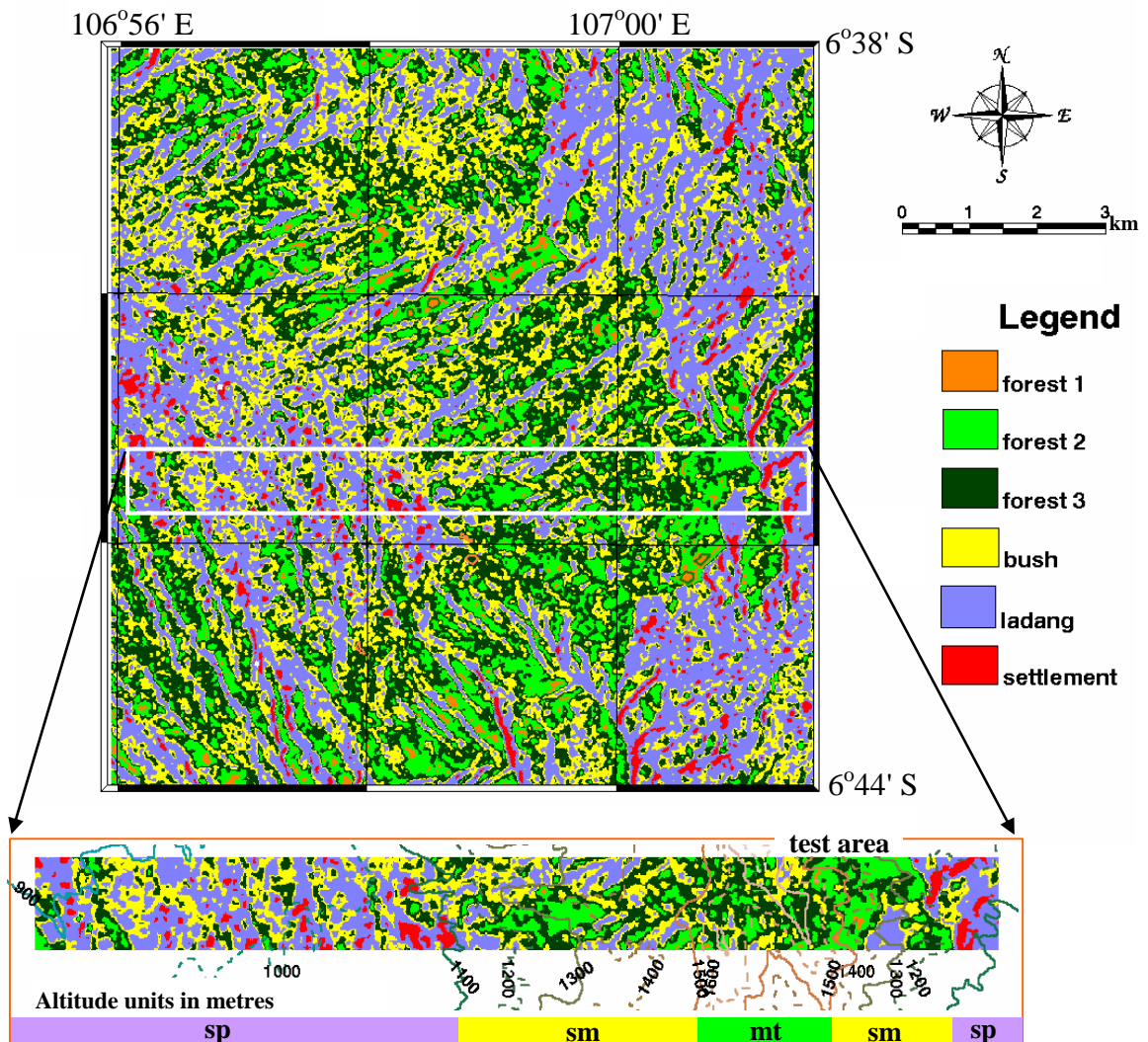


Figure 3.12. Classification result assigned the distribution of classes in the study area. Test area shows classes distribution in ecosystem zones and its terrain conditions. Ecosystem zones are settlement and paddy (sp), sub-montane (sm) and montane (mt).

Table 3.2. Relationship between backscattering coefficients and tree trunk diameters of rasamala forests in the study area

Class names	Backscattering coefficient (dB)	Trunk diameter (m)	Standard deviation (m)
forest 1	-12	0.290	0.0025
forest 2	-9	0.295	0.0025
forest 3	-7	0.300	0.0025

using 30 ground control points collected from topographic maps scale of 1:25 000 (BAKOSURTANAL 1990). This procedure yielded a geometric accuracy of 0.1 pixels. Then the spatial resolution of SAR image was resampled to 12.5m.

A supervised classification was performed to classify the data. The study area was classified into six classes based on topographic maps (BAKOSURTANAL 1990). They were namely forest 1, forest 2, forest 3, bush (tea), *ladang* (dry paddy fields), and settlement. Figure 3.12 shows classification results and the terrain characteristics of each ecosystem zone in the study area. The classification results contained only 1% error in comparison with the 30 training sites that were sampled from topographic maps. The terrain characteristics of the study area were generated using digital elevation model (DEM 1990). Figure 3.12 shows that forest classes distributed in the study area are at the altitude above 1100m or at the sub-montane and montane zones.

The statistical value of each forest class was derived and then the backscattering coefficient of each class was calculated using NASDA calibrated equation (Shimada 1998). These results are shown in table 3.2. Where the species included in forest classes in each pixel were assumed to be rasamala (*Altingia exelsa*), because it was the dominant species in the study area (refer Appendix F). By comparing the backscattering coefficient of each forest class to the curve of rasamala in figure 3.7, as seen in table 3.2, the trunk diameter of each forest class was obtained. This result shows that trees in sub-montane and montane tropical forest zones have a trunk diameter between 0.29m and 0.30m with standard deviation of each class is 0.0025m. These results matched well with the ground data.

3.6 Conclusions

Numerical analysis was conducted to analyse the relationship between the backscattering coefficients σ^o and diameter of tropical tree trunk. The analysis results were confirmed by simulation using Finite Difference Time Domain (FDTD) method. These results are in good agreement. A variation of this analysis, it could be applied to estimate diameter of tropical tree trunk from Synthetic Aperture Radar (SAR) data, which this information is very important to estimate the forest volumes effectively and accurately. These results succeeded in estimating tree trunk diameter of rasamala (*Altingia exelsa*) that is widely distributed in the Cisarua tropical forest, part of Gede Pangrango National Park, west Java, Indonesia (Tetuko *et*

al. 2001) from JERS-1 SAR data. While this study focused on single site in Indonesia, it is reasonable to expect that this method or variations should be successful in estimating tree trunk diameters in similar tropical forest regions of the world using SAR data.

References

1. BAKOSURTANAL, 1990, Topographic maps; Cisarua 1209-142, Gunung Hambalang 1209-144. Indonesian National Coordination Agency for Surveys and Mapping, 1st edn (Cibinong: BAKOSURTANAL).
2. DAVID, P., STELLA, E.B., STHEPHEN, J.M., 1997, Terrain influences on SAR backscatter around Mt. Taranaki, New Zealand. *IEEE Transactions on Geoscience and Remote Sensing*, 35, 924-932.
3. DEM, 1990, Digital Elevation Model: Cisarua 1209-142, Gunung Hambalang 1209-144. Indonesian National Coordination Agency for Surveys and Mapping, 1st edn (Cibinong: BAKOSURTANAL).
4. KAMAL SARABANDI, 1989, Electromagnetic Scattering from Vegetation Canopies, Ph.D Dissertation in the University of Michigan, Michigan: Michigan University.
5. LI, W., KOH, J., YEO, T., KOOI, P., 1999, "Analysis of Radiowave Propagation in a Four-layered Anisotropic Forest Environment," *IEEE Transactions on Geoscience and Remote Sensing*, vol.37, pp.1967-1979.
6. MUR, G., 1981, "Absorbing boundary Conditions for the finite-difference approximation of the time-domain electromagnetic-field equation," *IEEE Transactions on Electromagnetic Compatibility*, vol.23, no.4, pp.377-382.
7. SHIMADA, M., 1998, User's guide to NASDA's SAR products. Earth Observation

Research Centre (EORC), National Space Development Agency (NASDA), 2nd edn
(Tokyo: EORC-NASDA)

8. SUNAR, F., TABERNER, M., MAKTAV, D., KAYA, S., MUSAOGLU, M., and YAGIZ, E., 1998, The use of multi temporal radar data in agriculture monitoring: a case study in Kyocegiz-Dalaman ecosystem, Turkey. *International Archives of Photogrammetry and Remote Sensing*, 22, 559-565.
9. TETUKO S.S., J., TATEISHI, R., WIKANTIKA, K., 2001, "A method to estimate tree trunk diameter and its application to discriminate Java-Indonesia tropical forest," *International Journal of Remote Sensing*, vol. 22, no.1, pp.177-183.
10. UNO TORU, 1998, *Finite Difference Time Domain Method for Electromagnetic Field and Antenna Analyses*. 1st edition, Tokyo: Corona.
11. YEE, K. S., 1966, "Numerical solution of initial boundary value problems involving Maxwell's equations in isotropic media," *IEEE Transactions on Antennas Propagation*, vol.14, no.4, pp.302-307.